RECOIL EFFECTS IN PERIPHERAL NUCLEUS–NUCLEUS COLLISIONS AT $E/A = 84$ MeV

H.J. RABE, K.D. HILDENBRAND, U. LYNEN, W.F.J. MÜLLER [1], H. SANN, H. STELZER, W. TRAUTMANN, R. TROCKEL, R. WADA [2]
Gesellschaft für Schwerionenforschung, D-6100 Darmstadt, Fed. Rep. Germany

J. POCHODZALLA
Max-Planck Institut für Kernphysik, D-6900 Heidelberg, Fed. Rep. Germany and Institut für Kernphysik, D-6000 Frankfurt, Fed. Rep. Germany

E. ECKERT, P. KREUTZ, A. KÜHMICHEL
Institut für Kernphysik, D-6000 Frankfurt, Fed. Rep. Germany

N. BRUMMUND, R. GLASOW, K.H. KAMPERT, R. SANTO
Institut für Kernphysik, Universität Münster, D-4400 Münster, Fed. Rep. Germany

and

D. PELTE
Universität Heidelberg, D-6900 Heidelberg, Fed. Rep. Germany

Received 27 February 1987

Azimuthal angular correlations between projectile fragments and light particles have been measured in ^{18}O induced reactions on $^{58,64}Ni$ and ^{197}Au targets at $E/A = 84$ MeV. Neither sequential projectile decay nor evaporation from an equilibrated target-like recoil can explain the observed correlations. The data are well described in terms of a sideways-moving source suggesting emission of midrapidity light particles from a subset of nucleons which carries a major part of the transverse recoil momentum imparted by the projectile fragment.

Nucleus–nucleus collisions at intermediate energies, $E/A \approx 20$–200 MeV, are equally controlled by individual nucleon–nucleon collisions and collective mean field effects [1,2]. The concept of statistical, *random* emission from highly excited subsets of nucleons [3] has been rather successfully used to systematize the emission spectra of non-compound light particles [4]. Fission-frament–light-particle correlations [5], γ-polarization–light-particle correlations [1] and light-particle–light-particle correlations [2] suggest in addition an *ordered* transverse motion in the enetrance channel reaction plane. In the present work we investigate the interplay between random and collective mechanisms in peripheral reactions characterized by a projectile-like fragment emerging at forward angles. The observed azimuthal anisotropies of coincident light particles with respect to the leading projectile fragment can be parametrized in term of a sideways-moving source which carries a major part of the transverse recoil momentum imparted by the projectile fragment.

The experiment was performed at the CERN-SC.

[1] Present address: Lawrence Berkeley Laboratory, Berkeley, CA 94720, USA.
[2] Present address: Cyclotron Institute, Texas A&M University, College Station, TX 77843, USA.

^{58}Ni, ^{64}Ni and ^{197}Au targets of 1.1, 0.4 and 0.6 mg/cm^2 areal density, respectively, were bombarded with ^{18}O ions of $E/A=84$ MeV incident energy. Fragments emitted into an angular range of $2^\circ \leqslant \theta \leqslant 20^\circ$ were detected in a *zero-degree hodoscope* (ZDH). The inner part, $\theta \leqslant 6.5^\circ$, consisted of 18 plastic ΔE-scintillators of 5 mm thickness which were arranged in 3 concentric rings around the beam axis. Because of the narrow velocity distribution of projectile fragments emitted in this angular range [6,7], the energy loss signals were sufficient to determine the atomic number of the detected particles. The angular range from 6.5° to 20° was covered by 36 phoswich detectors (2 mm CaF_2 and 100 mm plastic scintillator). Particles detected in this part of the ZDH were identified by the ΔE–E technique with an energy threshold rising from 23 MeV for protons to $E/A \simeq 47$ MeV for ^{18}O nuclei. Coincident light particles emitted in the angular range $23^\circ \leqslant \theta \leqslant 78^\circ$ and $105^\circ \leqslant \theta \leqslant 157^\circ$ were detected in an array of 10 position sensitive 10 mm thick scintillators; the energy threshold was approximately $E/A \approx 3.5$ MeV. This *light-particle hodoscope* (LPH) covered a large solid angle of about 5.6 sr but did not allow particle identification. Isotopically resolved light particle distributions were measured with 5 telescopes positioned at $\theta = 40^\circ$, 51°, 63°, 73° and 120°. Each telescope consisted of three Si detectors (50 μm, 300 μm, 1000 μm) and a 10 mm thick BGO crystal.

We define the azimuthal correlation function, $R(\Delta\phi)$, in terms of the single and coincidence cross sections:

$$R(\Delta\phi) = C_{\mathrm{f},\ell\mathrm{p}} \frac{\sum \sigma_{\mathrm{f},\ell\mathrm{p}}}{\sum \sigma_{\mathrm{f}} \cdot \sigma_{\ell\mathrm{p}}} . \tag{1}$$

Here, σ_{f} denotes the production yield of a fragment (f) integrated over energy and solid angle of the corresponding detector element in the ZDH; $\sigma_{\ell\mathrm{p}}$ is the integral light particle (ℓp) yield measured in one LPH element and $\sigma_{\mathrm{f},\ell\mathrm{p}}$ is the corresponding coincidence cross section. For each laboratory angle of the fragment detector, θ_{f}, the sums in eq. (1) were performed over all detector pairs corresponding to a given azimuthal angle difference between the fragment and the light particle, $\Delta\phi$. $C_{\mathrm{f},\ell\mathrm{p}}$ is a normalization constant which was determined by the constraint $\langle R(\Delta\phi) \rangle = 1$.

Fig. 1. shows azimuthal correlation functions for several atomic charges and laboratory angles of the projectile fragments measured in reactions on Ni targets; in order to improve the statistics the data of the reactions on ^{58}Ni and ^{64}Ni were added together. To enhance the contributions from peripheral reactions only events with an observed associated charged particle multiplicity, $M_{\ell\mathrm{p}} \leqslant 2$, were selected in our analysis. The enhancement of the light ejectiles in the reaction plane, but in azimuthal direction opposite to the projectile fragment, $\Delta\phi = 180^\circ$, is apparent in all cases displayed in fig. 1. The magnitude of the enhancement is increasing with increasing charge and scattering angle of the leading fragment. To quantify these observations the correlation functions were fit with a function of the form

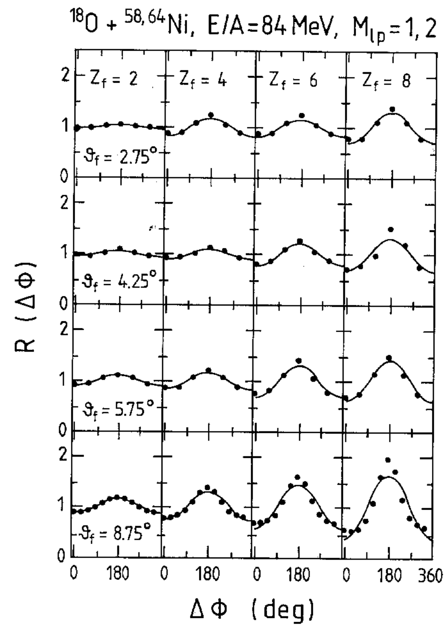

Fig. 1. Azimuthal correlation functions between fragments measured in the zero-degree hodoscope and particles detected in the light particle hodoscope for ^{18}O induced reactions on ^{58,64}Ni at $E/A = 84$ MeV. The curves are fits with eq. (2).

$$R(\Delta\phi) = 1 - \alpha \cos(\Delta\phi) . \tag{2}$$

The trends shown in fig. 1. suggest a relation between the enhancement, i.e., α, and the transverse momentum of the projectile fragment, $p_\perp = \beta_{\mathrm{f}} A_{\mathrm{f}} m_{\mathrm{N}} \sin(\theta_{\mathrm{f}})$, where β_{f} and A_{f} denote the frament velocity and mass number, respectively, and m_{N} is the nucleon mass. Since A_{f} and β_{f} were not directly measured in the

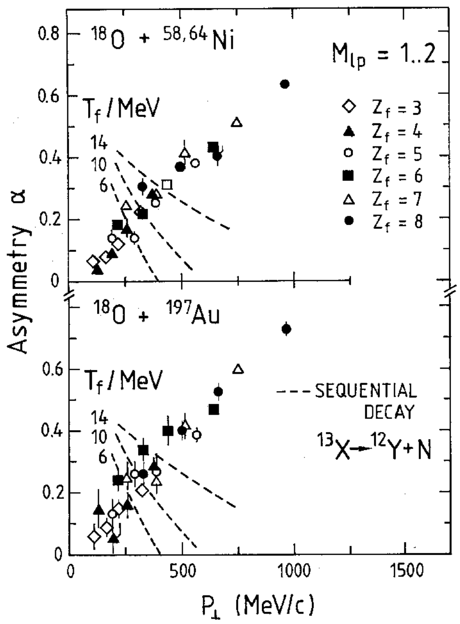

Fig. 2. Asymmetry parameter α [eq. (2)] as a function of the average transverse momentum of the projectile fragment.

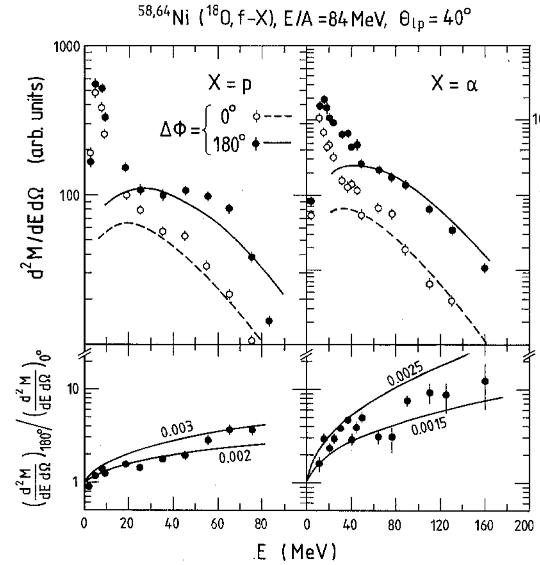

Fig. 3. Upper parts: Spectra of protons (left) and α-particles (right) measured at $\theta_{\ell p}=40°$ in coincidence with fragments of $6 \leqslant Z_f \leqslant 8$ in the zero-degree hodoscope for same side ($\Delta\phi=0°$) and opposite side ($\Delta\phi=180°$) emission. The solid and dashed lines are fits with the sideways-moving source parametrization of eq. (4). Lower parts: Opposite-side to same-side ratio. The curves are calculations with eq. (4). The numbers denote the values used for $\beta_\perp/T$ in MeV^{-1}.

experiment, we assumed the fragment mass to be given by $A_f=2Z_f$ and approximated the (average) fragment velocity by $\beta_f=\beta_{beam}g(\theta_f)$. Here β_{beam} denotes the beam velocity and $g(\theta_f)$ is a correction factor which takes the angular dependence of the mean fragment velocity into account (see e.g. ref. [7]). Consistent with the velocity distributions measured in the outer part of the ZDH we adopted in our analysis a simple linear relation $g(\theta_f)=1-\theta_f/100$, where θ_f is given in degrees. Fig. 2. shows the asymmetry parameter α as a function of $p_\perp$. Within the experimental uncertainties the relation between α and $p_\perp$ is linear and independent of the target nucleus.

The independence of the observed asymmetries on the size of the target nucleus already indicates that evaporation from equilibrated target-like recoils cannot explain the data: Because of the larger mass of the gold nucleus, its recoil velocity should be smaller for a given transverse momentum and, therefore, the anisotropy less pronounced. Another strong argument against target recoils being the main source of the observed asymmetry is given by the shapes of the coincident light particle spectra. As an example, the upper parts of fig. 3 show proton and α-particle spectra measured with the Ni targets at $\theta_{\ell p}=40°$ in coincidence with projectile fragments, $Z_f=6$–8. The shapes of these spectra are clearly inconsistent with the assumption of a single source having a temperature <10 MeV. The ratio of opposite-side to same-side emission (lower parts of fig. 3) show, that the major part of the azimuthal anisotropy is caused by a preequilibrium component which dominates at high energies.

To address the question whether the high energy part of the light particle spectra and hence the observed asymmetry is connected to the decay of excited projectile fragments we performed Monte Carlo calculations simulating the sequential decay of projectile fragments. The momentum distributions of the primary fragments were parametrized as [8,9]

$$\frac{d^3\sigma}{d\tilde{P}^3}=C\exp\left(-\frac{\tilde{P}_\perp^2}{2\tilde{\sigma}_\perp^2}\right)\exp\left(-\frac{(\tilde{P}_\parallel-P_0)^2}{2\tilde{\sigma}_\parallel^2}\right). \qquad (3)$$

For simplicity, the average longitudinal momentum, P_0, was fixed at a values corresponding to 95% of the beam velocity. The decay was assumed to be isotropic in the rest frame of the primary fragment; the decay energy spectrum was described in terms of a Maxwell–Boltzmann distribution $\rho(E) \propto \sqrt{E}\exp(-E/T_f)$. For a given temperature parameter T_f the *primary* longitudinal and transverse widths, $\tilde{\sigma}_\parallel$ and $\tilde{\sigma}_\perp$, were adjusted in order to reproduce the *secondary* longitudinal momentum width [6,9,10] and measured angular distribution of the projectile framents.

The dashed lines in fig. 2 indicate the results of these simulations for nucleon emission from mass 13 fragments. Temperature parameters of the order of $T_f \geqslant 10$ MeV are necessary in order to obtain anisotropies of similar magnitude as the experimental ones (cf. solid squares in fig. 2). Even higher temperatures are required in the case of α-fragment coincidences: e.g., a relative energy of at least 90 MeV is necessary to detect coincidences between α-particles at $\theta_{\ell p}=40°$ and beam velocity ^{12}C fragments in the ZDH for $\Delta\phi=180°$. These rather high temperatures together with the fact that for a given temperature the predicted azimuthal asymmetry decreases with increasing transverse momentum suggest that the observed correlations are not dominated by sequential decay of projectile fragments.

In order to determine the characteristics of the preequilibrium source we refer to a moving source parametrization. The light particles were assumed to be emitted isotropically in the rest frame of a source moving with a velocity $\beta_s=\sqrt{\beta_\parallel^2+\beta_\perp^2}$, where $\beta_\parallel$ and $\beta_\perp$ denote the velocity components parallel and transverse to the beam direction. The differential multiplicity spectrum in the laboratory system is then given by

$$\frac{d^2M}{dE\,d\Omega}=N\sqrt{E-E_c}\times\exp\{-[E-E_c+E_s-2\sqrt{(E-E_c)E_s}\cos\psi]/T\}\,. \quad (4)$$

Here E, E_c and $E_s=\frac{1}{2}A_{\ell p}m_N\beta_s^2$ are the laboratory energy of the light particle, the Coulomb repulsion by the target residue, and the energy due to the source velocity, respectively. ψ denotes the angle between the source velocity and the velocity of the light particle and N is a normalization constant. The opposite-side to same-side asymmetry, $\chi=(d^2M/dE\,d\Omega)(180°):(d^2M/dE\,d\Omega)(0°)$, then reads

$$\chi=\exp[\sqrt{2A_{\ell p}m_N(E-E_c)}\,\sin(\theta_{\ell p})\,\beta_\perp/T]\,. \quad (5)$$

Eq. (5) demonstrates that the anisotropy is mainly determined by $\beta_\perp/T$. The solid lines in the lower parts of fig. 3 show χ as a function of the energy calculated for different values of $\beta_\perp/T$. According to the experimental conditions, the calculations were averaged over a $\Delta\phi$ range of 60°. This $\Delta\phi$- averaging resulted in about 15% lower asymmetries as compared to eq. (5). It was verified that the choice of $\beta_\parallel$ has virtually no effect on χ. For simplicity, we neglected the Coulomb energy. Therefore, we will focus in the following discussion only on the high parts of the spectra, where this omission has no significant effect. Values of $\beta_\perp/T$ which are consistent with the observed asymmetries are listed in table 1.

In order to determine the temperature parameters, we fit the high energy parts of the light particle spectra with eq. (4). Unfortunately, the coincidence count rate in the more backward telescopes was too low to determine all parameters of the sources simultaneously. We, threfore, used the longitudinal source velocities which were extracted from a fit to the "inclusive" light particle spectra gated *only* on a light particle multiplicity $M_{\ell p}\leqslant 2$ [11] and neglected the Coulomb shifts. We then determined the temperature parameters and the normalization constants by fitting the high energy parts of the *coincident* light particle spectra at $\theta_{\ell p}=40°$ and using the relation between $\beta_\perp$ and T from table 1. The solid lines in the upper part of fig. 3 show the resulting fits; the extracted fit parameters are summarized in table 1.

Assuming that the transverse momentum imparted by the projectile fragment, $p_\perp$, is distributed among A_s nucleons representing the light particle source, the transverse velocity component of this source, $\beta_\perp$, and $p_\perp$ are due to momentum conservation [2] related according to

$$p_\perp=A_s m_N \beta_\perp\,. \quad (6)$$

Using the angle averaged transverse momenta of $Z_f=6$–8 fragments which were detected in coincidence with high energy particles ($E_p>15$ MeV and $E_\alpha>50$ MeV) and the transverse velocities listed in table 1, we can estimate the number of recoiling

Table 1
Parameters of the sideways-moving source [eq. (4)] for protons and α-particles emitted in ^{18}O induced reactions at $E/A=84$ MeV. $p_\perp$ is the average transverse momenta of the coincident projectile fragments with $Z_f=6$–8 and A_s denotes the apparent source sizes estimated with eq. (6).

Target	Particle	$\beta_\perp/T$ (MeV^{-1})	T (MeV)	$\beta_\parallel$	$\beta_\perp$	$p_\perp$ (MeV/c)	A_s
^{58,64}Ni	p	$(2.4+0.6)\times10^{-3}$	15 ± 2	0.18 ± 0.02	0.036 ± 0.010	350 ± 40	10 ± 3
	α	$(2.0\pm0.5)\times10^{-3}$	13 ± 2	0.16 ± 0.02	0.026 ± 0.008	360 ± 40	15 ± 5
^{197}Au	p	$(2.5\pm0.8)\times10^{-3}$	18 ± 2	0.21 ± 0.02	0.045 ± 0.015	340 ± 40	8 ± 3
	α	$(1.2\pm0.4)\times10^{-3}$	17 ± 2	0.14 ± 0.02	0.020 ± 0.007	370 ± 40	20 ± 7

nucleons [#1]: For intermediate-rapidity light particles (average) source sizes between 8 and 20 nucleons are found. Very similar values have recently been reported for ^{14}N induced reactions at $E/A=35$ MeV [12]. These small numbers are in line with the longitudinal source velocity for midrapidity light particles which typically amounts to half the beam velocity [11]. Both, the longitudinal and the transverse source velocities reflect the lacking ability of the target nucleus to absorb the incident momentum flow: Intermediate energy light particles seem to be emitted after only a few nucleon–nucleon interactions. There are, however, several problems which must be addressed in a more detailed and more quantitative discussion: (i) In each reaction a significant part of the transverse momentum may be transmitted via the Coulomb force between the incoming projectile or the outgoing fragment and the target-like nucleus. Due to the long-range nature of this interaction this transverse momentum will be distributed among the majority of all nucleons. (ii) Proximity effects, such as absorption phenomena [13] and Coulomb final state interactions [14] could modify the light particle distribution. However, we do not expect that more detailed calculations which include these effects will lead to a qualitative change in the interpretation of the observed correlations between projectile fragments and midrapidity light particles in peripheral nucleus–nucleus collisions in terms of the restriction of a significant part of the imparted transverse momentum to a subset of nucleons at the point of emission.

[#1] For simplicity, we assume that eq. (6) also holds for the average values, i.e. $\langle p_\perp\rangle=\langle A_s\rangle m_N\langle\beta_\perp\rangle$.

We are highly indebted to the staff of the CERN SC. This work was supported in part by the Bundesministerium für Forschung und Technologie.

References

[1] M.B. Tsang et al., Phys. Rev. Lett. 57 (1986) 559.
[2] C.B. Chitwood et al., Phys. Rev. C 34 (1986) 858.
[3] G.D. Westfall et al., Phys. Rev. Lett. 37 (1976) 1202.
[4] T.C. Awes et al., Phys. Rev. C 25 (1982) 2361.
[5] M.B. Tsang et al., Phys. Rev. Lett. 52 (1984) 1967.
[6] J. Mougey et al., Phys. Lett. B 105 (1981) 25.
[7] V. Borrel et al., Z. Phys. A 314 (1983) 191.
[8] A.S. Goldhaber, Phys. Lett. B 53 (1974) 306.
[9] K. Van Bibber et al., Phys. Rev. Lett. 43 (1979) 840.
[10] C.Y. Wong and K. Van Bibber, Phys. Rev. C 25 (1982) 2990.
[11] N. Brummund et al., Nucl. Phys. A 453 (1986) 349.
[12] B.A. Remington et al., Phys. Rev. C 34 (1986) 1685.
[13] H. Ho et al., Nucl. Phys. A 437 (1985) 465.
[14] J. Pochodzalla et al., Phys. Lett. B 175 (1986) 275.